



*Original Article*

## The effects of milling time on the synthesis of titanium diboride powder by self-propagating high temperature synthesis

Sutham Niyomwas<sup>1#\*</sup>, Narumon Chaichana<sup>2</sup>, Napisorn Memongkol<sup>3#</sup>,  
and Jessada Wannasin<sup>2#</sup>,

<sup>1</sup>Department of Mechanical Engineering,

<sup>2</sup>Department of Mining and Materials Engineering,

<sup>3</sup>Department of Industrial Engineering, Faculty of Engineering,

#NANOTEC Center of Excellence at Prince of Songkla University,  
Hat Yai, Songkhla, 90112 Thailand.

Received 28 September 2007; Accepted 8 May 2008

### Abstract

TiB<sub>2</sub> powders were obtained by self-propagating high-temperature synthesis from a mixture of TiO<sub>2</sub>, B<sub>2</sub>O<sub>3</sub> and Mg. The effect of milling duration of TiO<sub>2</sub> and B<sub>2</sub>O<sub>3</sub> to the resulted products was investigated. The products were characterized using X-ray diffraction and scanning electron microscope. Subsequently, the synthesized products were leached with 3.26 M HCl solutions and the final product of TiB<sub>2</sub> was obtained. The percentage of TiB<sub>2</sub> produced was affected by the milling time of TiO<sub>2</sub> and B<sub>2</sub>O<sub>3</sub>.

**Keywords:** titanium diboride, SHS, leach, milling

### 1. Introduction

TiB<sub>2</sub> is the most stable of the intermetallic compounds between the titanium (Ti) and boron (B) system. It has excellent properties, such as a high melting point (2970°C), high hardness (1800 Knoop), wear resistance of acids, and chemical inertness (Khanra *et al.*, 2004; Shi *et al.*, 2004; Gu *et al.*, 2003). Because of these excellent properties TiB<sub>2</sub> is used in many applications, such as ballistic armor, reinforced magnesium matrix composites, and cutting tools (Wang *et al.*, 2004; Jianxin *et al.*, 2005).

Recently, the TiB<sub>2</sub> synthesis process has attracted much attention and the successful processes to synthesize TiB<sub>2</sub> were preferred, such as the mechanical alloying of titanium

and boron powders, carbothermal reduction of titanium dioxide (TiO<sub>2</sub>) and boron oxide (B<sub>2</sub>O<sub>3</sub>), and the solid-state reaction of TiCl<sub>4</sub>, Mg, and MgB<sub>2</sub> (Hwang *et al.*, 2002; Krishnarao *et al.*, 2003)

A self-propagating high-temperature synthesis (SHS) method has been developed to produce ceramics, intermetallics, catalysts, and magnetic materials at low cost (Niyomwas, 2007; Suryanarayana, 2001; Millet *et al.*, 1996). This method exploits self-sustaining solid-flame combustion, which develops very high temperatures inside the materials over a short period. It therefore offers many advantages over traditional methods, such as a much lower energy loss, a lower environmental impact, a convenient manufacturing process, and unique properties of the product.

In the present study, TiB<sub>2</sub> powders were synthesized by the SHS method. The effect of milling duration of TiO<sub>2</sub> and B<sub>2</sub>O<sub>3</sub> to the resulted TiB<sub>2</sub> were investigated.

\*Corresponding author.

Email address: [sutham.n@psu.ac.th](mailto:sutham.n@psu.ac.th)

## 2. Experimental

The raw materials used in this study were  $\text{TiO}_2$ ,  $\text{B}_2\text{O}_3$  and Mg powder whose properties are listed in Table 1. The mole ratio of the precursor  $\text{TiO}_2:\text{B}_2\text{O}_3:\text{Mg}$  is 1:1:5. The experimental setup in this work is schematically represented in Figure 1. It consisted of a SHS reactor with a controlled atmospheric reaction chamber and tungsten filament connected to a power source through a current controller, which provides the energy required for the ignition of the reaction.

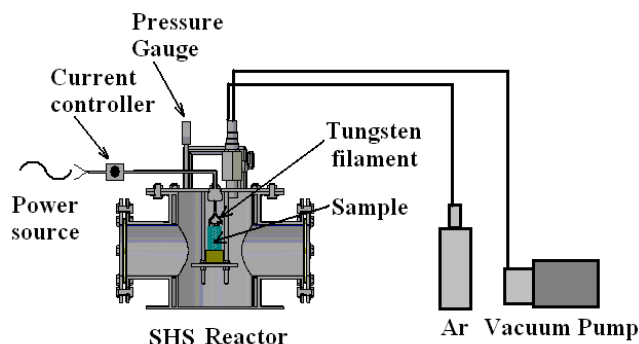


Figure 1. Schematic of the experimental setup.

$\text{TiO}_2$  and  $\text{B}_2\text{O}_3$  powder were weighted as stoichiometric ratio and milled in the planetary ball-milled (Tungsten jar and milling ball) with the speed 250 rpm for 0, 15, 30, 45 and 60 minutes, and milled with Mg powder for 15 minutes. The obtained mixture was uniaxially pressed to form cylindrical pellets (25.4 mm diameter) represented in Figure 2. The green sample was then loaded into the reaction chamber of the SHS reactor. The reaction chamber was evacuated with

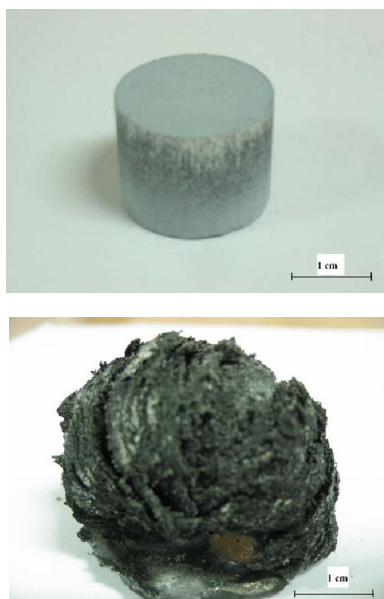


Figure 2. Photograph of (a) the green pellet of the precursors and (b) the synthesized product.

a vacuum pressure of 70 mmHg for 3 minutes and filled with Argon gas up to a pressure of 0.5 MPa. This operation was repeated at least twice in order to ensure an inert environment during the reaction revolution. A combustion front was generated at one sample end by using a heated tungsten filament. Then, under self-propagating conditions, the reaction front travels until it reaches the opposite end of the sample.

The obtained products were characterized in terms of chemical composition, surface morphology, and particle size by X-ray diffraction (PHILIPS X'Pert MPD), scanning electron microscope (JSM-5800LV, JEOL), and laser particle size analyzer (COULTER LS230), respectively

## 3. Results and Discussion

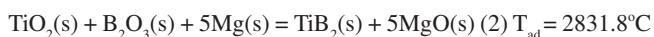
### 3.1 Thermodynamic Analysis

Calculations for the equilibrium concentration of stable species produced by the SHS reaction were performed based on the Gibbs energy minimization method (Gokcen and Reddy, 1996). The evolution of species was calculated for a reducing atmosphere and as a function of temperature, in the temperature range from 0 to 3000°C. Calculations assume that the evolved gases are ideal and form an ideal gas mixture, and the condensed phases are pure. The total Gibbs energy of the system can be expressed by the following equation:

$$G = \sum_{gas} n_i (g_i^o + RT \ln P_i) + \sum_{condensed} n_i g_i^o + \sum_{solution} n_i (g_i^o + RT \ln x_i + RT \ln \gamma_i) \quad (1)$$

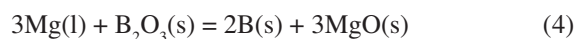
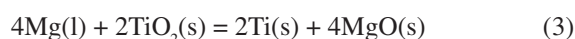
where,  $G$  is the total Gibbs energy of the system;  $g_i^o$  is the standard molar Gibbs energy of species  $i$  at  $P$  and  $T$ ;  $n_i$  is the molar number of species  $i$ ;  $P_i$  is the partial pressure of species  $i$ ;  $x_i$  is the mole fraction of species  $i$ ; and  $\gamma_i$  is the activity coefficient of species  $i$ . The exercise is to calculate  $n_i$  such that  $G$  is a minimized subject to the mass balance constraints.

The equilibrium composition of the  $\text{TiO}_2\text{-B}_2\text{O}_3\text{-Mg}$  system at different temperatures was calculated using Gibbs energy minimization method and the results are shown in Figure 3. The overall chemical reactions can be expressed as:



with  $T_{ad}$  is the adiabatic temperature of this reaction

During the SHS process,  $\text{TiO}_2$ ,  $\text{B}_2\text{O}_3$ , and Mg may have been interacted to form some possible compounds as following intermediate chemical reactions below show:



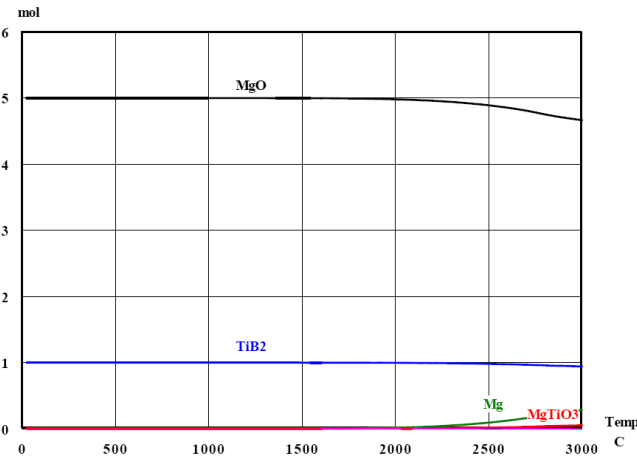


Figure 3. Equilibrium composition of  $TiO_2$ - $B_2O_3$ -Mg system in Ar gas atmosphere.

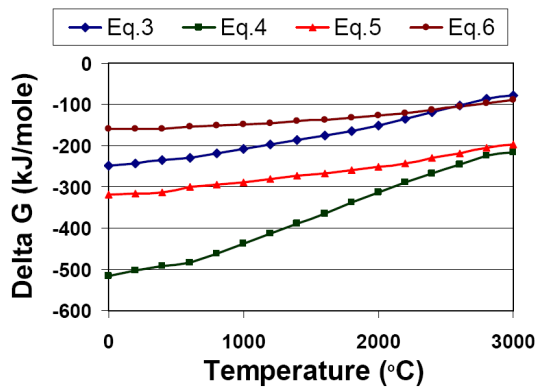


Figure 4. Gibbs Free Energy ( $\Delta G$ , in kJ/mole) of four different reactions (Equation 3, 4, 5, and 6, see text) at a temperature range from 0 to 3000°C.



Figure 3 reveals that it is thermodynamically feasible to synthesis composites by heat up the system of reaction (2). Accepting that, the reaction can be a self-sustained combustion, when the adiabatic temperature of the reaction is higher than 1800°C (Moore and Feng, 1992). Calculations have shown that the adiabatic temperature of the reaction system is higher than 1800°C, thus the use of SHS is feasible for this systems. Figure 4 shows that reaction (4) has the lowest

Gibbs energy of all four reactions. Mg reacts first with  $B_2O_3$ , then with  $TiO_2$  to yield elemental boron and titanium, which combined give  $TiB_2$ . Gibbs energy of reaction (5) (yields  $TiB_2$ ) is lower than that of reaction (6) (yields  $TiB$ ), which means that  $TiB_2$  is more stable than  $TiB$  over the whole temperature range.

A Differential Thermal Analysis (DTA) plot for the reactants mixture of  $TiO_2$ ,  $B_2O_3$ , and Mg powder is shown in Figure 5, with a heating rate of 10.0°C/min in the temperature range between 25 and 1300°C. The melting point of each reactant is listed in Table 1. Figure 5 shows an endothermic peak at 649.7°C, which corresponds to the melting point of Mg at 650°C. The exothermic peak at 728.4°C corresponds to the reaction of melted Mg with oxide phases as indicated in Equation (3) and (4).

### 3.2 Effect of milling duration of $TiO_2$ and $B_2O_3$ to the precursor mixture.

The particles size of the milled products was analyzed by a laser particle size analyzer (LPSA) as shown in Figure 6. The mean particle size decreased after a milling time of 15 minutes, then it showed agglomeration of the particles after a milling time of 30 minutes. Further milling resulted again in a decrease of the particle size (after 45 minutes) and after 60 minutes agglomeration of the particles can be seen again. The overall trend of the milling process shows a decrease of the mean particle size with increasing milling time. However, one obvious difference with increasing milling time was the decrease of submicron-scale particles from a milling time of 15 to 60 minutes.

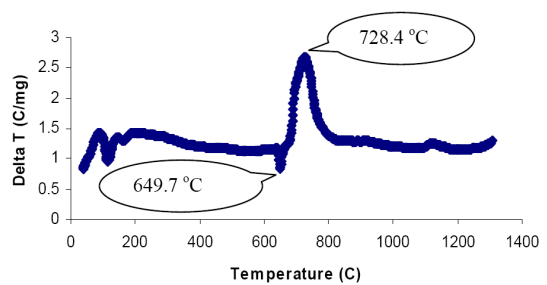


Figure 5. Differential thermal analysis (DTA) plot of a mixture of  $TiO_2$ ,  $B_2O_3$ , and Mg powders with a heating rate of 10°C/min.

Table 1. Properties of the reactant powders.

| Reactant | Vendor                                   | Purity (%) | Particle size ( $\mu m$ ) | Melting point ( $^{\circ}C$ ) |
|----------|--|------------|---------------------------|-------------------------------|
| $TiO_2$  | Asia Pacific Specialty Chemicals Limited | 79.9       | 36.71                     | 1,843                         |
| $B_2O_3$ | Aldrich Chemical Company, Inc.           | 99         | 1017                      | 450                           |
| Mg       | Riedel-deHaen                            | 99         | 267                       | 650                           |

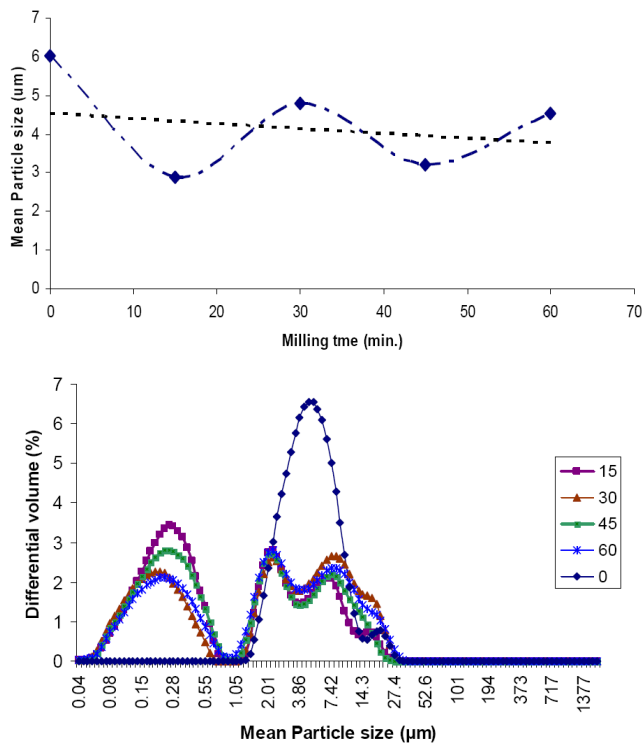


Figure 6. (a) Relation between milling time and mean particle size of  $TiO_2+B_2O_3$  mixture and (b) the mean particle size distribution.

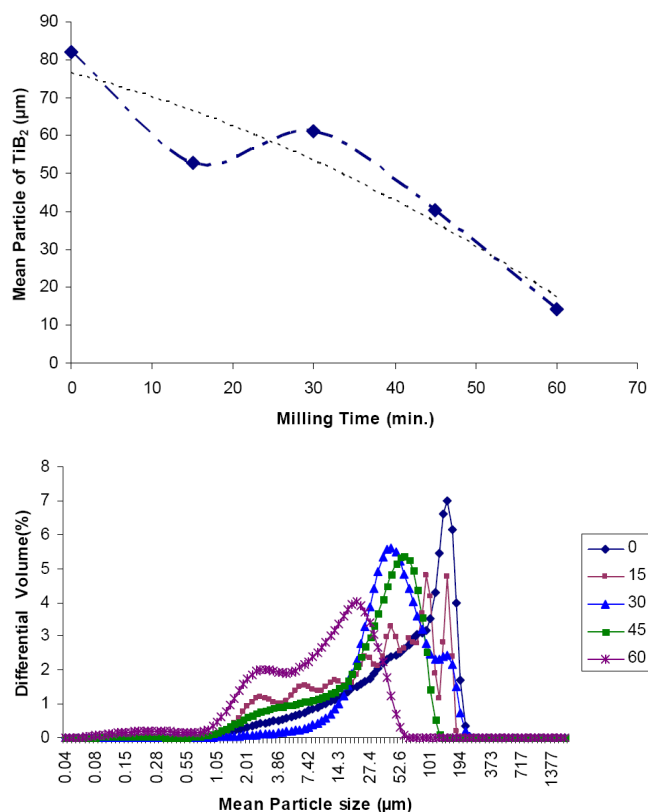


Figure 7. (a) Relation between milling time and mean particle size of  $TiB_2$  and (b) the mean particle size distribution.

### 3.3 Effect of milling time duration on the synthesized product

The particles size of  $TiB_2$  after leaching was analyzed by LPSA as shown in Figure 7. The size range of  $TiB_2$  particles is much larger than of the starting materials. This may caused by the agglomerated of submicron-sized  $TiB_2$  particles shown in Figure 10. The particle size of  $TiB_2$  was reduced with increasing milling time. Whereas, the weight percent of  $TiB_2$  increases as the milling time increases to 45 minutes, but then after 60 minutes the weight percentage dropped. The effect of the milling time to the synthesized product is shown in Table 2 and Figure 8. This outcome might have been the result of a larger surface area for reaction and higher absorbed energy from the milling process. The reasons why the  $TiB_2$  weight percentages decreased after 60 minutes milling of the precursor are not yet clear.

After the synthesis, the powder was leached out with a 3.26M HCl solution for 48 hours and the phases were then identified with XRD. Figure 9 shows the XRD patterns of the typical products before and after the leaching process in which  $MgO$  and  $Mg_2TiO_4$  were leached out leaving only the final product of  $TiB_2$ . Figure 10 shows SEM micrographs of products from the SHS reaction before and after the leaching

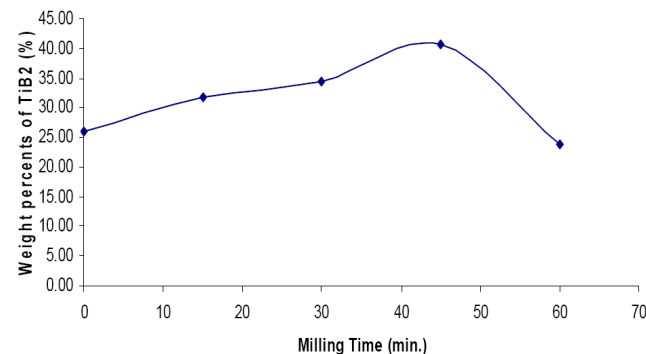


Figure 8. Relation between milling time and weight percent of  $TiB_2$  after leaching.

Table 2. The weight of the powder before and after leaching and the weight percent of  $TiB_2$  at different milling times.

| Milling Time (min.) | Weight of synthesized powder before leached (g) | Weight of synthesized powder after leached (g) | Weight of $TiB_2$ after leached (%) |
|---------------------|---|--|-------------------------------------|
| 0                   | 12.01   | 3.12   | 25.98                               |
| 15                  | 9.01  | 2.87   | 31.85                               |
| 30                  | 12.01   | 4.13   | 34.36                               |
| 45                  | 12.01   | 4.87   | 40.55                               |
| 60                  | 15.00   | 3.58   | 23.88                               |

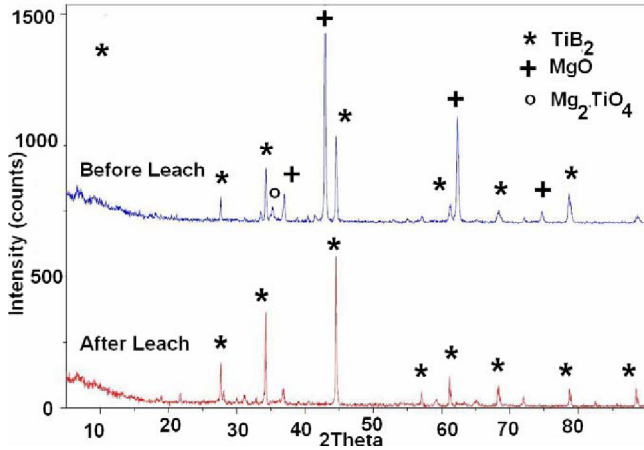


Figure 9. XRD patterns of a typical product from before and after the leaching process (here the sample is taken after a milling time of 15 minutes).

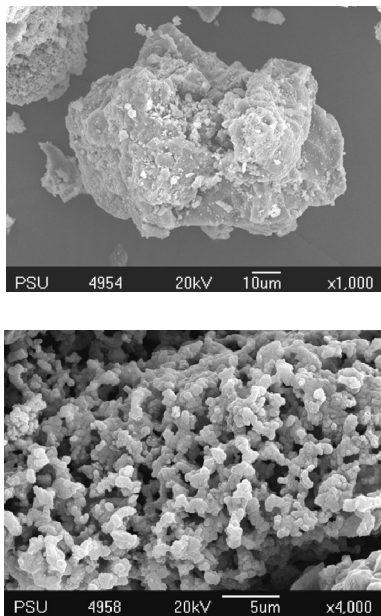


Figure 10. SEM images of the SHS products from (a) before leaching and (b) after leaching.

process. The morphology of the products before the leaching process shows an agglomerate of oxide compounds ( $MgO$  and  $Mg_2TiO_4$ ) and  $TiB_2$ . However, after the leaching the SEM picture reveals good inter-particle cohesion of the  $TiB_2$  particles as identified in the XRD patterns in Figure 9. Figure 11 shows the XRD patterns of the leached products from the precursors at the different milling times of 0, 15, 30, 45 and 60 minutes. A small amount of  $MgO$  was still left in the leached product from the precursor in the 30 minutes milling time sample.

These resulted phases of the products match well with the thermodynamic model proposed as shown in the XRD patterns of Figure 9 and 11. Nevertheless, the formation of the intermediate phase of  $Mg_2TiO_4$  shows that the reaction of

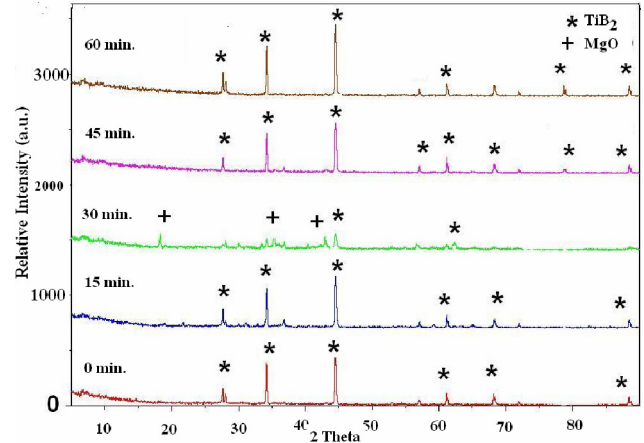
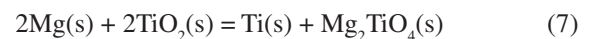


Figure 11. XRD patterns of the leached products from the precursors at different milling time, 0, 15, 30, 45 and 60 minutes.

Equation (3) was incomplete. This may be due to the higher temperature of reaction ( $>2000^\circ C$ ), which favors the decomposition of  $MgO$  to  $Mg$  as shown in Figure 3. The additional detailed reduction stages for Equation (3) may be written as:



#### 4. Conclusions

The in-situ synthesis of  $TiB_2$  was produced through self-propagating high-temperature synthesis reaction from precursors of  $TiO_2$ - $B_2O_3$ - $Mg$  with a mole ratio of 1:1:5. The increase of the milling time of the precursors from 0 to 45 minutes resulted in higher weight percentages of  $TiB_2$ , from 25 to 40.

#### Acknowledgements

The authors are pleased to acknowledge the financial support from the National Nanotechnology Center (NANOTEC), NSTDA, Ministry of Science and Technology, Thailand, through its "Program of Center of Excellence Network" (NANOTEC Center of Excellence at Prince of Songkla University), and partial financial support from the Ceramic and Composite Materials Research Group (CMRG) of the Faculty of Engineering, Prince of Songkla University, Thailand

#### References

- Gokcen, N.A. and Reddy, R.G. 1996. Thermodynamic, Plenum Press, New York, NY, U.S.A., pp. 291-294.
- Gu, Y., Qian, Y., Chen, L. and Zhou, F. 2003. A mild solvo-thermal route to Nanocrystalline titanium diboride. Journal of Alloys and Compounds. 352, 325-327.
- Hwang, Y. and Lee, J. K. 2002. Preparation of  $TiB_2$  power by mechanical alloying. Materials Letters. 5, 1-7.

- Jianxin, D., Tongkun, C. and Lili, L. 2005. Self-lubricating behaviors of  $Al_2O_3/TiB_2$  ceramic tools in dry high - speed machining of hardened steel. *Journal of European Ceramic Society*. 25, 1073-1079.
- Khanra, A.K., Mishra, L.C. P., and Godkhindi, M.M. 2004. Effect of NaCl on the synthesis of  $TiB_2$  powder by a self-propagation high-temperature synthesis technique. *Materials Letters*. 58, 733-738.
- Krishnarao, R.V. and Subrahmanyam, J. 2003. Studies on the formation of  $TiB_2$  through carbothermal reduction of  $TiO_2$  and  $B_2O_3$ . *Materials Science and Engineering A*. 362, 145-151
- Millet, P. and Hwang, T. 1996. Preparation of  $TiB_2$  and  $ZrB_2$  influence a mechano-chemical treatment on the borothermic reaction of titanium and zirconia. *Journal Materials Science*. 31, 351-355.
- Moore, J.J. and Feng, H.J. 1995. Combustion Synthesis of Advanced Materials: Part I. Reaction Parameters. *Progress in Materials Science*. 39, 243-273.
- Niyomwas, S. 2007. Synthesis of porous composite by self-propagating high temperature synthesis of  $TiO_2-B_2O_3-Al$  system. EPD Congress 2007, The Annual Meeting of The Minerals, Metal & Materials Society (TMS), Orlando, FL, U.S.A., Feb 25-Mar 1, 2007, 261-170.
- Suryanarayana, C. 2001. Mechanical Alloying and milling. *Journal of Materials Science*. 46, 1-184.
- Shi, L., Gu, Y., Chen, L., Yang, Z., Ma, J. and Qain, Y. 2004. A convenient solid-state reaction route to nanocrystalline  $TiB_2$ . *Inorganic Chemistry*. 7, 192-194.
- Wang, H.Y., Jiang, Q.C., Zhao, Y.Q., Ma, B.X. and Wang, Y. 2004. Fabrication of  $TiB_2$  and  $TiB_2-TiC$  particulates reinforced magnesium matrix composites. *Materials Science and Engineering A*. 372, 109-114.